AeroEagles

Mathematical Model Report — Part 1

Vedarsh Mishra, Lucas DiMarco and Devin Dear,

March 12, 2026

1. Introduction

1.1 General Importance of Research Area

In May 2015, SpaceX successfully landed a Falcon 9 first-stage booster, establishing rockets as multi-use aircrafts and reducing the cost of access to orbit significantly. NASA's Space Shuttle required approximately $1.5 billion per launch for low-earth orbit. On the other hand, the reusable Falcon 9 operates at roughly $62 million per mission [1]. That 24-fold cost reduction was achieved almost entirely through one capability: autonomous powered vertical landing. The rocket guides itself back to the ground, decelerates under its own thrust, and lands precisely enough to fly again.

Most model rockets rely on a fundamentally different approach: passive parachute recovery. A parachute deploys near apogee and the vehicle drifts back to the ground with no directional control, susceptible to wind drift, and frequently sustaining structural damage on landing. This project asks a direct question: can the principles behind the Falcon 9's landing system be demonstrated at model-rocket scale, using off-the-shelf components built in a university makerspace? The purpose of this report is to answer this question using rigorous mathematical modeling of each subsystem.

1.2 Project Architecture

The AeroEagles system has two principal components. The first is a standard model rocket which is a PVC-bodied vehicle launched on a commercial solid-propellant motor, targeting approximately 1000 meters of altitude. The second is a landing module that mounts to the aft end of the rocket and activates autonomously at apogee. The landing module contains two coupled subsystems:

Pneumatic attitude control system: compressed-air jets mounted offset from the rocket's center of mass fire in response to tilt angle errors, generating corrective torques that keep the vehicle body axis aligned with vertical during descent.

Propeller guidance system: a quad-rotor propeller arrangement generates controllable horizontal thrust to steer the vehicle laterally toward a pre-designated landing target. The goal is landing within a five-foot (1.52 m) radius.

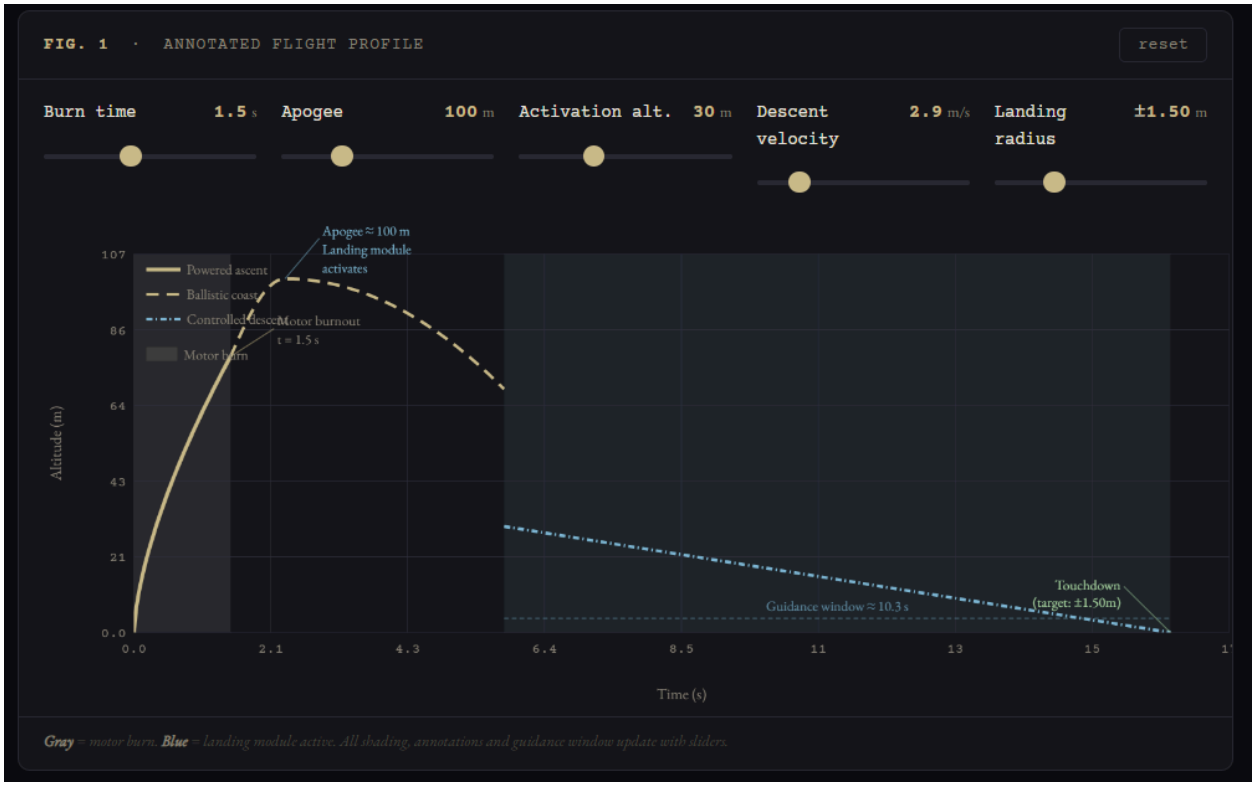


Figure 1. Annotated flight profile for the AeroEagles self-landing rocket.

1.3 Scope of This Report

This report develops mathematical models for four aspects of the system: (1) vertical flight dynamics and force balance during controlled descent; (2) propeller deployment dynamics, including motor spin-up and residual angular momentum dissipation; (3) attitude stabilization using the pneumatic PID control system; and (4) horizontal position guidance using the propeller PID control system. For each subsystem, we derive governing equations, identify parameters, apply the models numerically, and discuss the assumptions and uncertainties involved.

2. Background Research

2.1 Rocket Flight Mechanics

A rocket in vertical flight is governed by four forces: thrust (F_T), weight ($W = mg$), aerodynamic drag (F_D), and a lateral aerodynamic force in a non-zero wind. During powered ascent, thrust exceeds weight and the rocket accelerates upward. After motor burnout at approximately $t = 1.5$ s, the vehicle enters a ballistic coast phase, decelerating under gravity and drag until it reaches apogee. In our system, apogee is the moment the landing module activates.

The aerodynamic drag force on a body moving through air scales with the square of velocity. This quadratic dependence means a rocket falling twice as fast experiences four times the drag,

and that there exists a terminal velocity at which drag exactly balances gravity. For our rocket in the deployed landing module configuration, the passive terminal velocity is approximately 16.7 m/s which is fast enough to destroy the vehicle on impact. Active propeller braking reduces this to a safe controlled descent speed [2].

2.2 Rotational Dynamics and Attitude

The attitude of a rocket is its orientation in space, specifically the angle between its body axis and the vertical. During descent, any tilt angle θ produces two problems: it reduces guidance effectiveness by rotating propeller thrust vectors away from horizontal, and it allows the vehicle to drift laterally. Maintaining an attitude as close to vertical as possible is essential to landing accuracy.

The physics of rotation for a rigid body are governed by Euler's equation: net torque equals moment of inertia times angular acceleration [3]. The moment of inertia characterizes how difficult it is to angularly accelerate a body, and it depends on both total mass and the distribution of that mass relative to the rotation axis. A long rocket with mass concentrated far from the rotation axis has a high moment of inertia and requires larger torques to correct its attitude.

2.3 PID Control Theory

A proportional-integral-derivative (PID) controller is the dominant feedback control architecture in industrial and aerospace engineering, used in systems ranging from automotive cruise control to the attitude thrusters on the International Space Station. A PID controller computes a control output as the weighted sum of three terms based on a measured error signal e(t) [4].

The **proportional term** (K_P* e) responds immediately to the current error. The **derivative term** (K_d*de/dt) responds to how fast the error is changing, providing damping and preventing overshoot. The **integral term** ($K_i \int e\, dt$) accumulates error over time, eliminating steady-state offset. The gains K_P, K_i, and K_d are design parameters that determine the speed, stability, and accuracy of the closed-loop system.

2.4 Propeller Thrust and Motor Dynamics

Propeller thrust arises from the momentum change imparted to air passing through the rotor disk. In the operating regime of small drone-scale motors, thrust is approximately proportional to the square of motor rotational speed (RPM). This quadratic relationship means that thrust builds slowly during spin-up: even when the motor reaches 80% of target RPM, it only produces 64% of maximum thrust [5]. This is a critical design constraint for the deployment sequence.

2.5 Angular Momentum at Apogee

A model rocket in flight typically acquires a slow axial spin due to the cant angle of its stabilizing fins. This spin, on the order of 30 RPM (3.14 rad/s), is present at apogee when the landing module activates. From the rocket's perspective, this represents stored angular momentum that must be dissipated before attitude control can operate cleanly. An often overlooked constraint is if attitude correction is attempted before this spin is removed, gyroscopic coupling will cause the vehicle to precess rather than correct [6].

3. Mathematical Model Development

3.1 Vertical Flight Dynamics

We model the rocket as a point mass in one-dimensional vertical motion. During the descent phase, when the landing module is active and the motor is burned out, the net vertical force is the sum of gravity (downward), aerodynamic drag (upward), and active propeller braking thrust (upward). Applying Newton's second law:

$$[\text{A}]\ ma = \ -\ mg\ +\ \tfrac{1}{2}\rho v^2 C_D A\ +\ F_{brake}$$

Equation [A]: Net force during controlled descent

where m is total mass, a is vertical acceleration (positive upward), g = 9.81 m/s², ρ is air density, v is descent speed, C_D is the drag coefficient of the deployed configuration, A is effective drag area, and F_{brake} is propeller braking thrust. Setting a = 0 gives the *controlled descent velocity*:

$$[\text{B}]\ v_{descent} = \sqrt{\frac{2(mg - F_{brake})}{(\rho C_D A)}}$$

Equation [B]: Equilibrium controlled descent velocity (with braking)

$$[\text{C}]\ v_{T.V.\,descent} = \sqrt{\frac{2mg}{(\rho C_D A)}}$$

Equation [C]: Terminal velocity descent (no breaking)

Using the parameters in Table 1 with F_{brake} = 4.0 N, equation [B] gives a controlled descent velocity of approximately **2.9 m/s**, compared to a passive terminal velocity of **16.7 m/s** from equation [C]. The active braking system reduces impact speed by a factor of nearly six. Figure 2 illustrates the force balance across the full range of descent speeds.

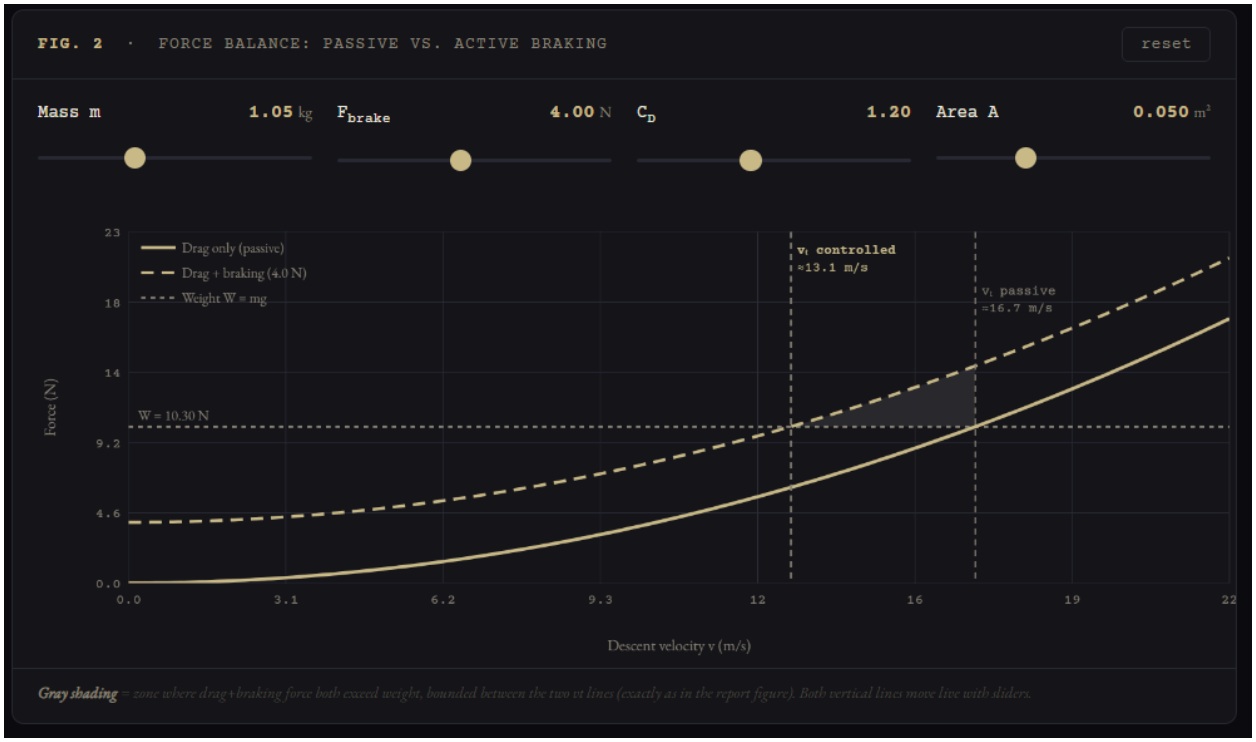


Figure 2. Force balance during descent. Solid: passive aerodynamic drag only.

3.2 Propeller Deployment Dynamics

The propeller system does not reach full thrust instantaneously. When the deployment command is issued at apogee, the motors must spin up from rest, and the propeller arms must physically unfold and lock. Both processes introduce lag that must be accounted for in the landing sequence.

3.2.1 Motor Spin-Up

The rotational speed of a brushless DC motor in response to a step throttle command follows a first-order exponential approach governed by a mechanical time constant τ_{spinup}. The motor angular velocity $\omega(t)$ and thrust $F_{thrust}(t)$, which scales as ω^2, are:

$$[D]\ \omega(t) = \omega_{max}(1 - e^{-t/\tau})$$

Equation [D]: Motor spin-up (first-order)

$$[E]\ F_{thrust}(t) = F_{max}(\omega(t)/\omega_{max})^2$$

Equation [E]: Thrust force with RPM

With $\tau_{spinup} \approx 0.25$ s, the motors reach 95% of maximum RPM in approximately 0.75 s, but only 40% of maximum thrust at t = 0.25 s (since thrust scales as ω^2). This means **motors must begin**

spinning approximately 0.5–0.75 s before apogee so full braking thrust is available from the start of controlled descent.

3.2.2 Residual Spin Dissipation

The residual axial spin acquired during ascent must be dissipated before attitude control can operate cleanly. The spin-down dynamics are governed by aerodynamic drag torque. For a spinning cylindrical body, the drag torque is proportional to the square of spin rate, giving:

$$[\mathrm{F}]\ I_{axail}\frac{d\Omega}{dt} = \ -\ k\Omega^{2}$$

Equation [F]: Axial spin down equation of motion

where I_{axail} is the axial moment of inertia, Ω is the spin rate, and k is an aerodynamic drag coefficient. We additionally propose using the propellers as active counter-torque actuators: commanding props to rotate opposite to the rocket's spin generates a counter-torque that dissipates angular momentum approximately 3 times faster than passive drag alone. Figure 3 shows both the spin-up profile and spin dissipation comparison.

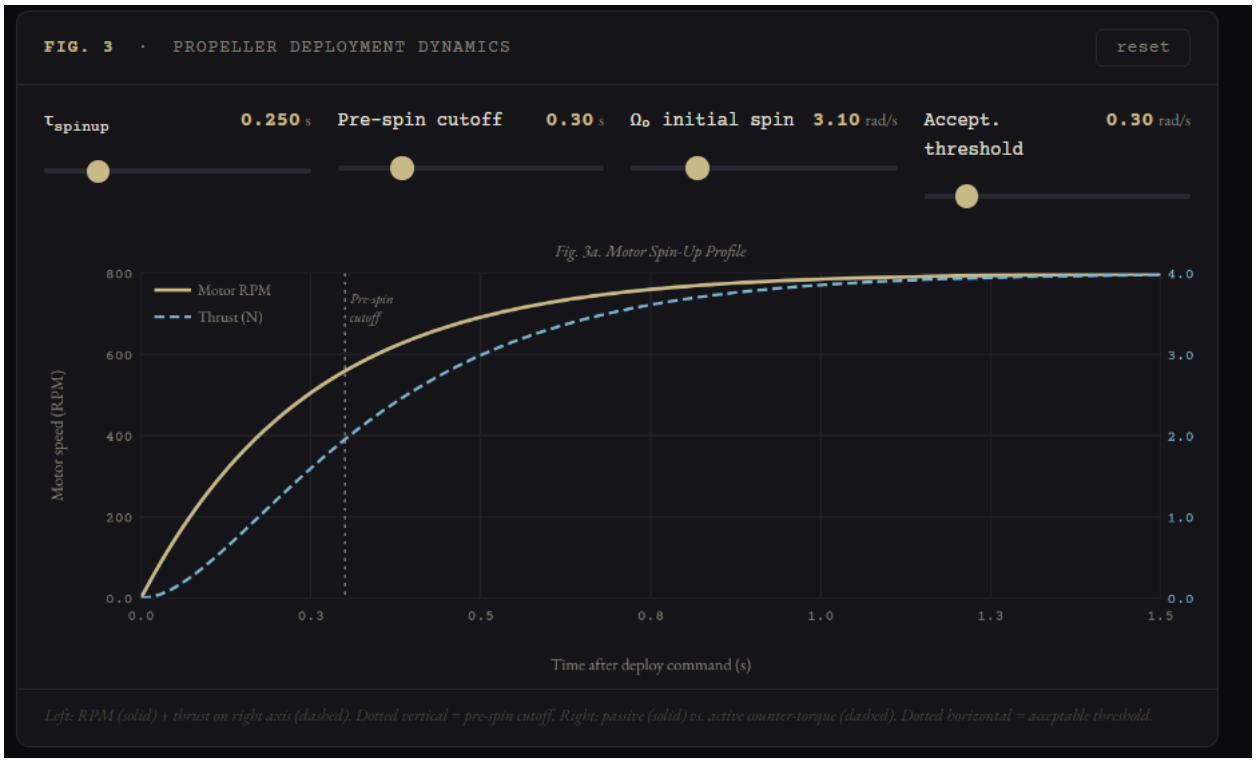


Figure 3. Propeller deployment dynamics. motor spin-up profile showing RPM (solid) and generated thrust (dashed).

3.3 Attitude Control Model (Pneumatic System)

We define tilt angle θ as deviation of the rocket's body axis from vertical, in radians. For θ < 15°, we apply the small-angle approximation (sin θ ≈ θ), which linearizes the equations of motion. Euler's rotational equation about the transverse axis through the center of mass is:

$$[G]\ I_{cm}\theta^{(2)} = \tau_{net}$$

Equation [G]: Euler's rotational equation

$$[H]\ \tau_{net} = -mgr_{cm}\theta + F_{jet}d_{arm}$$

Equation [H]: Net torque for small angles

$$[I]\ \tau_{cmd}(t) = K_p e + K_i \oint e dt + K_d\left(\frac{de}{dt}\right)$$

Equation [I]: PID torque command (e(t) = -θ(t))

$$[J]\ I_{cm}\theta^{(2)} = -mgr\theta + d_{arm}\left(K_p e + K_i \oint e + K_d e\right)$$

Equation [J]: Full closed-loop attitude dynamics

Figure 4 shows the simulated tilt response using nominal PID gains from Table 1, along with a gain sensitivity analysis. The model predicts settling within ±2° in approximately 0.23 s, well within any descent time budget.

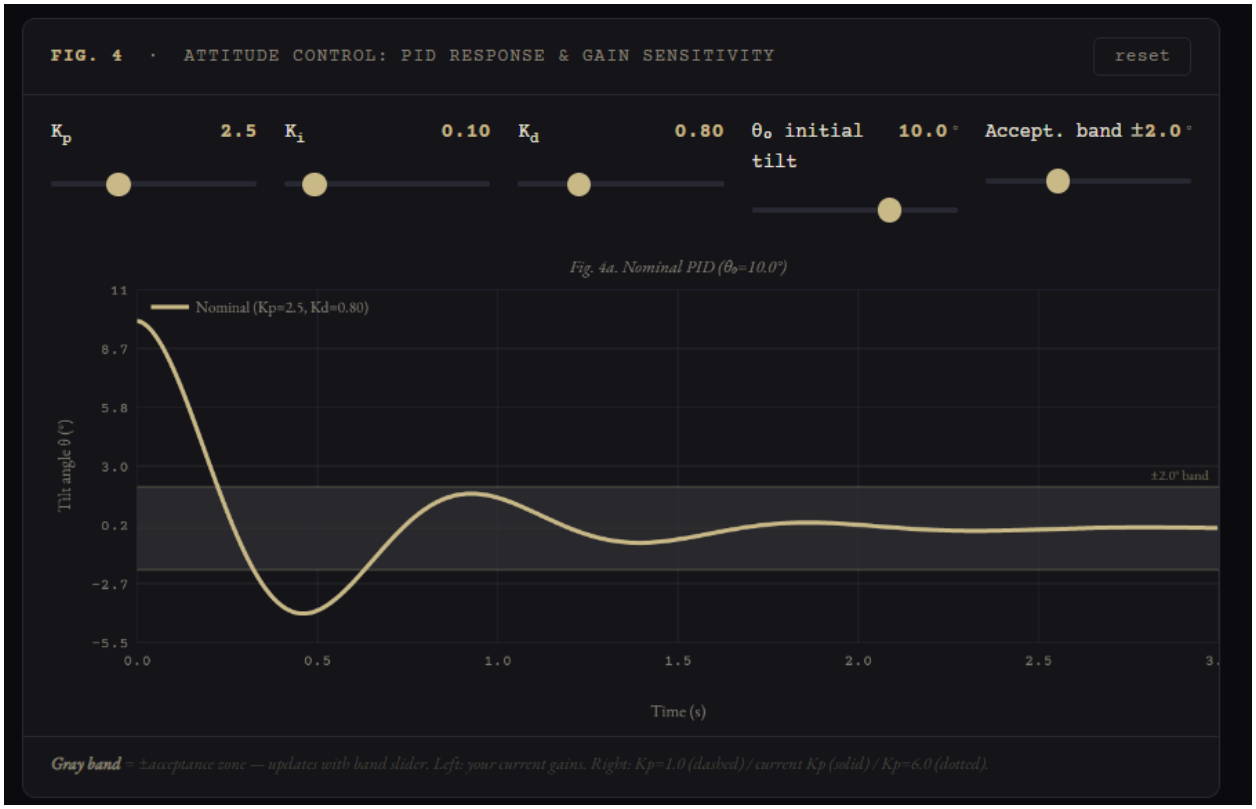


Figure 4. Attitude control simulation.

3.4 Horizontal Guidance Model (Propeller System)

Let x(t) denote horizontal distance from the target. The equation of motion under propeller thrust and horizontal aerodynamic drag is:

$$[\mathrm{K}]\ mx^{(2)} = F_{prop}(t) - bx^{(1)}$$

Equation [K]: Horizontal dynamics under thrust and drag

$$[\mathrm{L}]\ F_{cmd}(t) = -(K_p x + K_i \oint x dt + K_d x^{(1)})$$

Equation [L]: PID guidance force command

$$[\mathrm{M}]\ |F_{cmd}| \leq F_{max}$$

Equation [M]: Thrust saturation constraint

$$[\mathrm{N}]\ t_{avail} = \frac{h}{v_{descent}}$$

Equation [N]: Available descent correction window

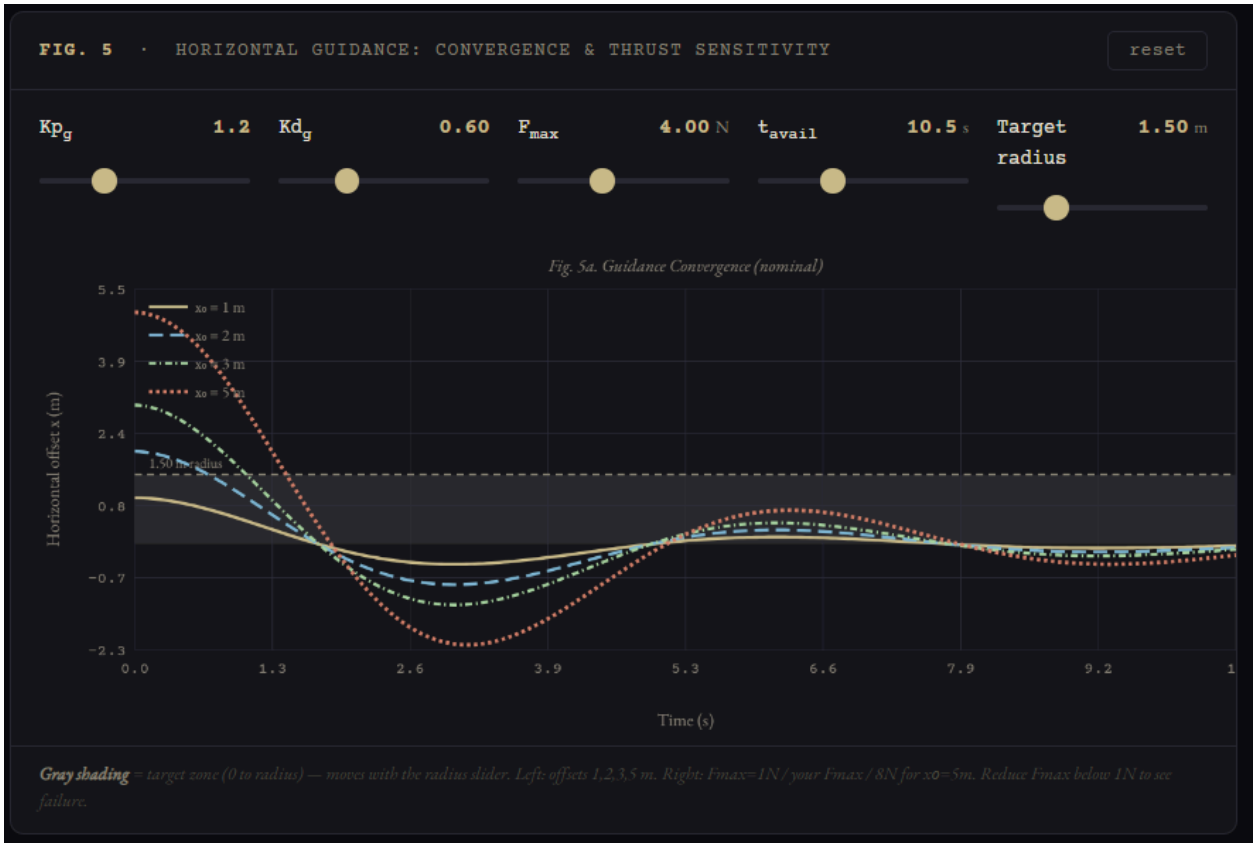


Figure 5. Horizontal guidance simulation.

3.5 Coupling Between Subsystems

The attitude and guidance subsystems are physically coupled: a tilt angle θ reduces horizontal thrust effectiveness by cos θ, and horizontal acceleration perturbs attitude through an inertial torque. For $\theta < 15°$, $\cos(15°) \approx 0.966$ which is a less than 4% reduction in guidance thrust. We therefore adopt the decoupled model as our primary analysis tool, with the explicit acknowledgment that large-tilt behavior ($\theta > 15°$) requires the full nonlinear coupled equations.

4. Model Parameters

Table 1 summarizes all physical constants and design parameters used across the models in Section 3. Parameters marked "to be measured" or "to be tuned" carry the largest uncertainty and are the primary targets of the spring validation campaign described in Section 6. The drag coefficient will be measured using the Boston College wind tunnel; the moment of inertia via bifilar pendulum; and the PID gains through iterative drop testing.

Table 1. Physical constants and design parameters for the AeroEagles landing module models.

Symbol / Quantity	Value	Units	Source / Notes
m (dry mass)	0.85	kg	Estimated; PVC body + electronics
m_total (w/ motor)	1.05	kg	Estes C6-5 installed
g	9.81	m/s²	Standard sea-level
C_D (deployed config)	1.20	—	Bluff body; prop arms deployed
A (eff. drag area)	0.050	m²	~20 cm prop span deployed
rho (air density)	1.225	kg/m³	Sea level, 15°C
I_cm	0.042	kg·m²	Thin-rod estimate — to be measured
L (length)	0.60	m	Full assembly estimate
d_arm	0.20	m	Pneumatic nozzle moment arm
tau_spinup	0.25	s	Motor mechanical time constant
omega_rocket (apogee)	3.14	rad/s	Fin-cant induced spin (~30 RPM)
F_prop per motor	0.5 – 2.0	N	Quad config; throttle-dependent
F_brake (max total)	4.0	N	4 motors, vertical braking
Kp (attitude)	2.5	—	PID nominal — to be tuned
Ki (attitude)	0.10	—	PID nominal — to be tuned
Kd (attitude)	0.80	—	PID nominal — to be tuned
Kp (guidance)	1.2	—	PID nominal — to be tuned
Kd (guidance)	0.60	—	PID nominal — to be tuned

> ***On uncertainty:*** *Several parameters, particularly C_D, I_{cm}, τ_{spinup}, and all PID gains, are estimated rather than measured. A 20% error in I_{cm} shifts the attitude settling time by ~10%, which is acceptable at this design stage. These uncertainties are the inputs to our spring testing campaign.*

5. Interactive Parameter Explorer

The mathematical models in Section 3 are implemented as a live interactive web application (*AeroEagles_Explorer.html*) that allows any user to modify system parameters and observe the effect on model predictions in real time. The explorer contains three tabbed modules: descent dynamics, attitude control, and horizontal guidance. Each of these with parameter sliders, live-updating animated charts, and real-time display of key performance metrics.

The file runs entirely in any modern web browser without installation. Key demonstrations: drag K_P above 6 to observe PID instability; reduce F_{max} below 1 N to see guidance failure; adjust activation altitude to change the available descent window.

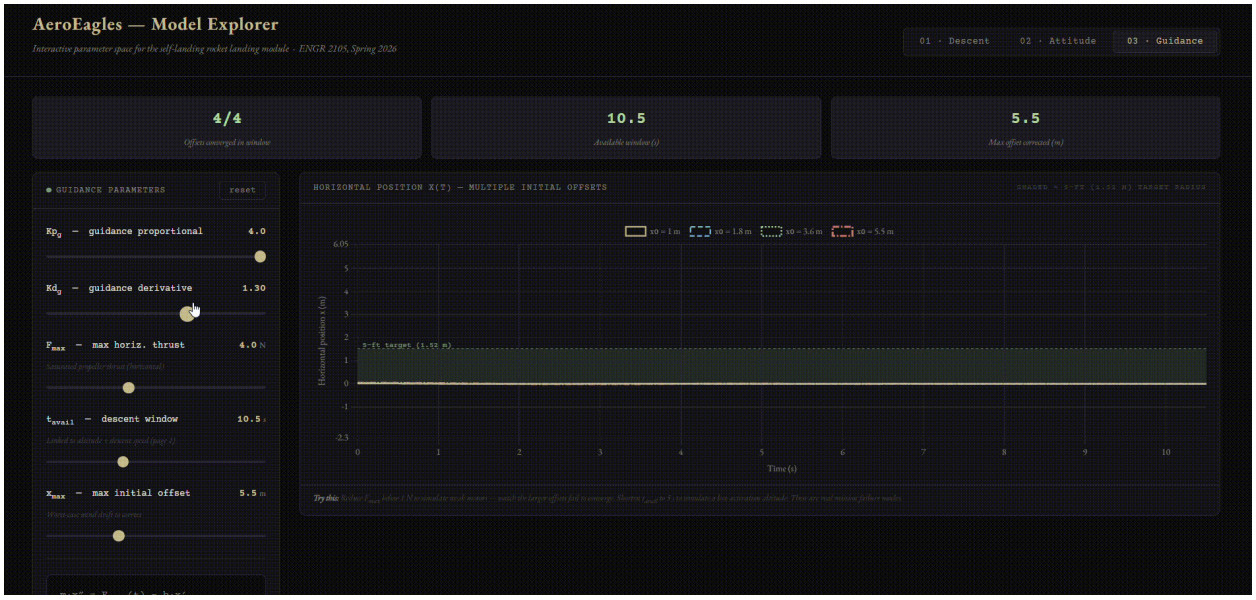


Figure 6. Linking to the AeroEagles Interactive Model Explorer. Open AeroEagles_Explorer.html in any browser to interact with live parameter sliders and animated charts for all three subsystem models.

6. Conclusion

This report has developed a comprehensive mathematical framework for the AeroEagles self-landing rocket system across four interconnected subsystems, deriving fourteen governing equations and generating quantitative predictions for each.

The **descent dynamics model** (equations [A]–[C]) demonstrates that active propeller braking reduces the descent speed from a vehicle-destroying 16.7 m/s to a manageable 2.9 m/s — a factor-of-six reduction that is the enabling capability of the entire system.

The **deployment dynamics model** (equations [D]–[F]) identifies a critical constraint: motors must begin spinning approximately 0.5–0.75 s before apogee so that full braking thrust is available at activation. Residual axial spin from fin cant must also be actively dissipated; using the propellers as counter-torque actuators reduces this time by ~3 times.

The **attitude control model** (equations [G]–[J]) predicts that the pneumatic PID system can reject a 10° tilt disturbance and return to within $\pm 2°$ in approximately 0.23 s. The gain sensitivity analysis confirms K_P must remain below ≈5 to avoid oscillatory instability.

The **horizontal guidance model** (equations [K]–[N]) predicts that even a 5 m initial position offset — our worst-case wind drift estimate — can be corrected within the 10.3 s descent window, meeting the 5-foot landing radius specification. Below ≈1 N of maximum thrust, the system fails to converge.

The limitations of this analysis are clearly stated: all PID gains, the drag coefficient, moment of inertia, and motor time constant are estimated rather than measured. The decoupled subsystem model is valid only for $\theta < 15°$. These are not deficiencies, rather they are the concrete inputs to our spring validation campaign.

Next steps: three baseline launches in March to measure actual descent velocity; bench testing of motor spin-up dynamics; and progressively higher instrumented drop tests of the landing module. Each test produces data that directly updates the models in this report.

7. Bibliography

[1] Wikipedia, "Falcon 9 First-Stage Landing Tests," Wikimedia Foundation, 2024. [Online]. Available: https://en.wikipedia.org/wiki/Falcon_9_first-stage_landing_tests

[2] M. Poli et al., "Autonomous Re-entry System Technology Demonstrator for Sounding Rockets," in 2016 IEEE Metrology for Aerospace (MetroAeroSpace), Jun. 2016, pp. 439–443. doi: 10.1109/MetroAeroSpace.2016.7573255.

[3] H. Goldstein, C. Poole, and J. Safko, Classical Mechanics, 3rd ed. San Francisco, CA: Addison-Wesley, 2002, pp. 134–180.

[4] K. J. Åström and T. Hägglund, PID Controllers: Theory, Design, and Tuning, 2nd ed. Research Triangle Park, NC: ISA, 1995.

[5] L. Su, J. Wang, Z. Ma, and H. Chen, "Real-time Guidance for Powered Landing of Reusable Rockets via Deep Reinforcement Learning," in 2022 IEEE ICUS, Oct. 2022, pp. 214–219. doi: 10.1109/ICUS55513.2022.9986540.

[6] J. W. Sonderegger, "Vertical Take-Off and Landing Control via Dual-Quaternions and Sliding Mode," M.S.E.P., Embry-Riddle Aeronautical University, 2022.

[7] C. Wang and Z. Song, "Trajectory Optimization for Reusable Rocket Landing," in 2018 IEEE CSAA CGNCC, Aug. 2018, pp. 1–6. doi: 10.1109/GNCC42960.2018.9019105.

[8] R. Linsen et al., "Optimal Thrust Vector Control of an Electric Small-Scale Rocket Prototype," in 2022 IEEE ICRA, Philadelphia, PA, 2022, pp. 1–7.

[9] Estes Industries, "Estes C6-5 Motor Technical Specifications," 2023. [Online]. Available: https://www.estesrockets.com\

[10] G. J. Blaney and D. R. Holder, "Drag Coefficients for Cylinders at Subsonic Velocities," NASA Technical Note TN D-1540, NASA, 1963.

Equation List:

[A] (Net Force/Newton's Second Law): This fundamental physics principle explains how force equals mass times acceleration (F=ma). Newton's Second Law of Motion

[B] & [C] (Terminal Velocity): These equations describe the point where drag and thrust balance gravity to reach a constant descent speed. Terminal Velocity Equation Explained

[D] (Motor Spin-up Time Constant): A guide on how mechanical time constants govern the speed response of DC motors. DC-Motor Calculations & Parameters

[E] (Thrust vs. RPM): This research highlights the quadratic relationship where thrust increases with the square of the rotational speed. Propeller Performance Curves

[F] (Aerodynamic Drag Torque): Technical analysis of the torque experienced by rotating bodies in a fluid. Aerodynamic Torque on a Rotating Disc

[G] (Euler's Rotational Equation): The standard equations used to describe the rotation of a rigid body. Euler's Equations for Rigid Body Dynamics

[H] (Small Angle Approximation): A mathematical tool used to simplify trigonometric functions for control models. Small Angle Approximations

[I] & [L] (PID Control Law): A detailed explanation of how proportional, integral, and derivative terms combine to manage error. PID Theory Explained

[J] (Closed-Loop Dynamics): Documentation on how feedback systems stabilize a process. Closed-Loop Control Techniques

[K] (Horizontal Motion with Drag): Mathematical modeling of projectiles or vehicles moving horizontally through air. Projectile Motion with Air Resistance

[M] (Thrust Saturation): While specific to hardware, the concept of saturation in control systems is summarized here. PID Controllers & Saturation

[N] (Descent Correction Window): An application of basic kinematics for objects falling with air drag. Projectile with Air Drag Dynamics